

## Raman study of the $\alpha \rightarrow \beta$ structural phase transition of solid $N_2$

G. Pangilinan, G. Guelachvili,\* R. Sooryakumar, and K. Narahari Rao  
*Department of Physics, The Ohio State University, Columbus, Ohio 43210*

R. H. Tipping

*Department of Physics and Astronomy, University of Alabama, Tuscaloosa, Alabama 35487*

(Received 14 July 1988)

Raman spectra of solid  $N_2$  have been obtained at small temperature intervals in the range 4 to 40 K. Relative intensities of both the low-frequency lattice modes and the higher-frequency vibrational stretching modes have been measured with a spectral resolution of approximately  $2 \text{ cm}^{-1}$ . In addition to changes associated with the structural transition between a low-temperature ordered cubic ( $\alpha$  phase) and a high-temperature hcp lattice ( $\beta$  phase) at  $T_c = 35.6 \text{ K}$ , we report a dramatic evolution of the Raman intensity with temperature within the  $\alpha$  phase, and present evidence for a partial relaxation of the orientational ordering approximately 10 K below  $T_c$ . The results support the existence of a "plastic phase" within the  $\alpha$  phase, near the  $\alpha$ - $\beta$  phase boundary.

### I. INTRODUCTION

Many molecular solids display transitions from an orientationally ordered (hindered rotation) to an orientationally disordered (precession or free rotation) phase, a process that is governed, at least in part, by electrostatic interactions between the molecules.<sup>1-3</sup> In solid  $N_2$  for example, at  $T = T_c = 35.6 \text{ K}$  there is a phase transition from the cubic low-temperature ordered  $\alpha$  phase to the hcp orientationally disordered  $\beta$  phase.<sup>1</sup> Numerous theoretical studies of the intermolecular potential, the multipole and short-range interactions, of these solids have appeared and several bulk properties in the different phases hence predicted.<sup>1,2,4-6</sup> While the harmonic approximation is often adequate for lattice-dynamic calculations, in solid  $N_2$ , however, anharmonic effects are important.<sup>7</sup> In this situation a perturbation approach has been sufficient in many instances.<sup>8</sup> Unfortunately, close to a phase transition, the molecular motions are enhanced and hence such an approximate description would become inadequate.

The molecular-dynamics method has been used to simulate solid  $N_2$  in the  $\alpha$  phase.<sup>6</sup> This model revealed that the  $\alpha$  phase is in fact subdivided into two zones. For temperatures well below the  $\alpha$ - $\beta$  coexistence line, orientational order exists and the molecules perform librational motion about a mean direction—as expected in the  $\alpha$  phase.<sup>1</sup> In the second zone, a few degrees below  $T_c$ , the molecules on the fcc lattice do not have a well-defined orientation. The predicted structure of solid  $N_2$  in this zone is hence that of a "plastic" crystal. However, due to a lack of experimental evidence for this new phase,<sup>6</sup> the order parameters characterizing the  $\alpha$ - $\beta$  transition have been generally accepted as first order.<sup>1</sup>

Numerous experimental studies of solid  $N_2$  have been carried out and the salient results of these works have been reviewed by Scott.<sup>1</sup> Raman spectra of both the low-frequency lattice modes and the higher-frequency

stretching modes have been obtained for samples both in the  $\alpha$  and  $\beta$  phases.<sup>9-14</sup> Most of these experimental studies, however, were conducted at a constant temperature or at several temperatures within one of the distinct phases. In this paper, we present results of a systematic Raman study of solid  $N_2$  across the  $\alpha$ - $\beta$  structural transition.

Because of the alteration in lattice structure and concomitant symmetry selection rules, changes in both the positions and intensities of various lines were expected and observed for the two phases. In addition, we report on two new findings that provide indirect evidence of the plastic phase that appears as a precursor to the structural transition. The first relates to the dramatic changes in intensity of several Raman transitions with small temperature changes in the  $\alpha$  phase. In addition, variations in the wings of both the lattice and stretching lines that occur about 10 K below  $T_c$  are consistent with the occurrence of plastic behavior. These results near the phase boundary, hence provide insight into the behavior of the orientational order parameter that is dominated by the build up of large amplitude librational motions of the molecules with temperature.

In the following section we give a description of the experimental setup used to grow large solid samples, and to control and monitor the temperature. Details associated with the measurement of the spectra and the experimental results are presented in Sec. III. Discussion of these results is provided in the final section.

### II. EXPERIMENTAL SETUP

Solid  $N_2$  was grown *in situ* in a specially designed cell, shown in Fig. 1, and mounted inside an optical cryostat. Nitrogen gas was introduced into the cell at about 60 K, where it condenses into a clear liquid. Three heaters  $R_1$ ,  $R_2$ , and  $R_3$  are mounted at different positions in the cell;  $R_1$  ensures that no solidification would obstruct passage

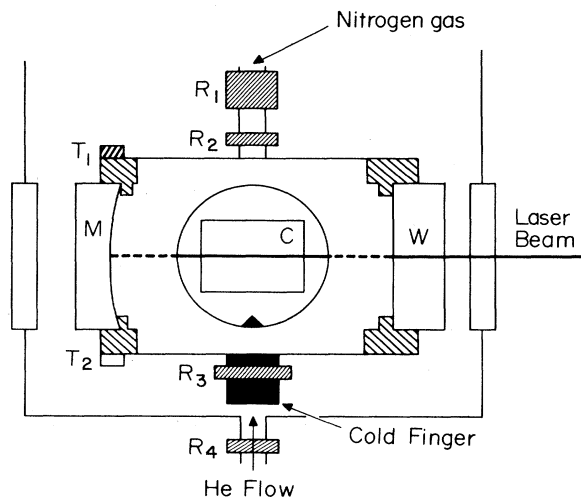


FIG. 1. Schematic diagram of the Raman cell and its components when installed inside cryostat. *C* is the cylindrical mirror at the inner backside of the cell as seen from the collection window. It refocusses radiation scattered symmetrically with respect to the right-angle scattering geometry. The heaters  $R_i$ , thermal sensors  $T_i$ , and mirror *M* are described in the text.

of the gas, while  $R_2$  and  $R_3$ , mounted on the top and bottom of the cell, allow its direct heating. A copper cold finger extends from the bottom and emerges with a pointed tip protruding slightly into the interior of the cell. The higher thermal conductivity of the finger provides an effective means of preferentially cooling it in relation to the rest of the cell. This feature results in the solid beginning its crystallization at the cold tip. To avoid cracks, the crystal is then cooled very slowly for about 3 h towards the transition temperature. Once grown the solid is stable and, in one measurement, a crystal was maintained for more than 20 h.

To exploit the optimum homogeneity of the crystal, the laser beam (150 mW of 5308-Å radiation) is incident near its center along a horizontal axis. Several steps were taken to maximize the measured signals. These included double passing the beam through the cell by having a spherical mirror *M* that reflects back the incident photons, refocusing the radiation scattered symmetrically with respect to the conventional right-angle collection geometry, and the rotation of the vertical slit image by  $90^\circ$  to match the vertical slits of the monochromator. These steps proved vital in our ability to detect several subtle and weak features in the Raman spectra that is central to this work.

Particular care was placed on knowing the absolute crystal temperature. The cell temperature was monitored by two diodes  $T_1$  and  $T_2$  calibrated to within  $\pm 0.1$  K and placed at the top and bottom of the cell as in Fig. 1. For each spectrum the temperature  $T_{av}$  was evaluated by averaging temperatures  $T_1$  and  $T_2$  before and after each scan. Since minimal laser heating was also expected, the temperatures measured may differ from that of the region being excited. The absolute temperature is obtained since

it is known that the  $\alpha$ - $\beta$  transition occurs at 35.6 K at normal pressures. The temperature  $T$  is then determined from  $T = T_{av} + \text{constant}$ . By assigning  $T = 35.6$  K for the scan (see Fig. 4) which exhibited the phase transition, the constant was found to be 0.6 K in our measurements. The overall error in the calculation of  $T$  is estimated to be about  $\pm 0.25$  K.

### III. RESULTS

The measurements concentrated on two spectral regions: the intramolecular stretching-mode regime, 2200–2500  $\text{cm}^{-1}$ , and the lower-frequency lattice region to about 150  $\text{cm}^{-1}$ . Many scans were in the 38–32 K temperature range bordering the phase transition. Additional measurements were made within the  $\alpha$  phase to 3.6 K. The evolution of the spectra was followed from the  $\beta$  to the  $\alpha$  phase.

#### A. Stretching-mode region

Figures 2(a) and 2(b) show the spectral features near the interatomic stretching frequency as a function of temperature. The vibrational frequency has symmetry  $A_g + T_g$  in the  $\alpha$  phase and  $A_{1g}$  in the  $\beta$  phase.<sup>1</sup> Of particular interest is the approximate threefold enhancement in intensity between scans at 18.2 and 26.1 K [Fig. 2(a)]. The intensity then decreases slightly at the elevated temperatures of 33.6 and 34.6 K just below  $T_c$ . Upon reaching the  $\beta$  phase at  $T = T_c$ , there is a small abrupt intensity increase that shows further modest growth up to  $T = 37$  K. The frequency of the stretching mode remains unchanged from 3.6 to about 18.2 K before gradually decreasing by  $0.3 \text{ cm}^{-1}$  just below  $T_c$ . A sudden decrease in frequency of  $0.6 \text{ cm}^{-1}$  occurs upon crossing to the  $\beta$  phase.

Figure 2(b) shows the temperature dependence of weaker structures in these energy range. Comparing the spectra around  $T_c$  at 35.4 and 35.9 K, one sees the abrupt emergence of wings on the sides of the  $A_{1g}$  mode that signals the transition to the  $\beta$  phase. The wings appear

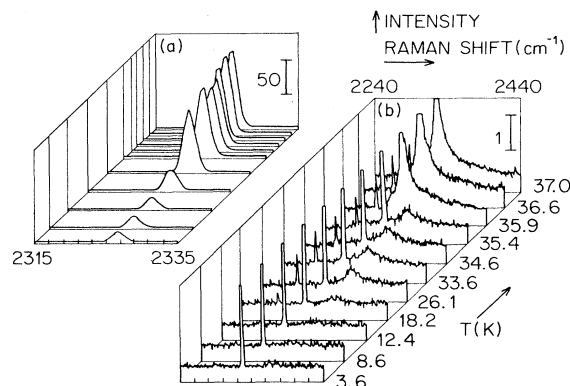


FIG. 2. (a) Temperature dependence of the Raman modes near the stretching frequency. (b) Raman spectra highlighting weaker features near stretching frequency as a function of temperature. The numbers next to the bars indicate the relative intensity scales, 50 and 1, for (a) and (b), respectively. The resolution was  $2 \text{ cm}^{-1}$ .

asymmetric. Careful examination of the data, as evident from Fig. 3, reveals in addition to the main peaks, the successive appearance with increasing temperature, of three weak broad features designated as *A*, *B*, and *C* respectively. Components *A* and *B* are present in both  $\alpha$  and  $\beta$  phases while *C* appears only in the  $\beta$  phase. *B* is a weak broad ( $\sim 100 \text{ cm}^{-1}$  wide) structure that is first observed around 30 K. The feature *C* is about 50 times less intense than the narrow line of the stretching mode centered also at  $2326 \text{ cm}^{-1}$ . We find that the spectral profile of the wings of the narrow stretching mode in the  $\beta$  phase spectrum at 35.9 K is well represented by the sum  $A + B + C$ .

The broader weak feature (*A*) around  $2360 \text{ cm}^{-1}$  is seen in five spectra of Fig. 2 starting at  $T = 18.2 \text{ K}$ . We identify this as a combination of stretching and lattice modes. The narrow mode at  $2288 \text{ cm}^{-1}$  is identified as the  $^{15}\text{N}^{14}\text{N}$  isotopic stretching mode. The intensity of this mode is about 130 times weaker than the normal isotopic peak, in agreement with the measured isotopic abundance ratio.

#### B. Lattice modes

Figures 4(a) and 4(b) exhibit the spectra in the low-energy lattice region. The features near  $32 \text{ cm}^{-1}$  ( $E_g$ ) and  $37 \text{ cm}^{-1}$  ( $T_g$ ) in the  $\alpha$  phase have been identified as crystal-field split librational modes.<sup>11</sup> The strong  $E_g$  mode in the  $\alpha$  phase and its absence in the  $\beta$  phase is

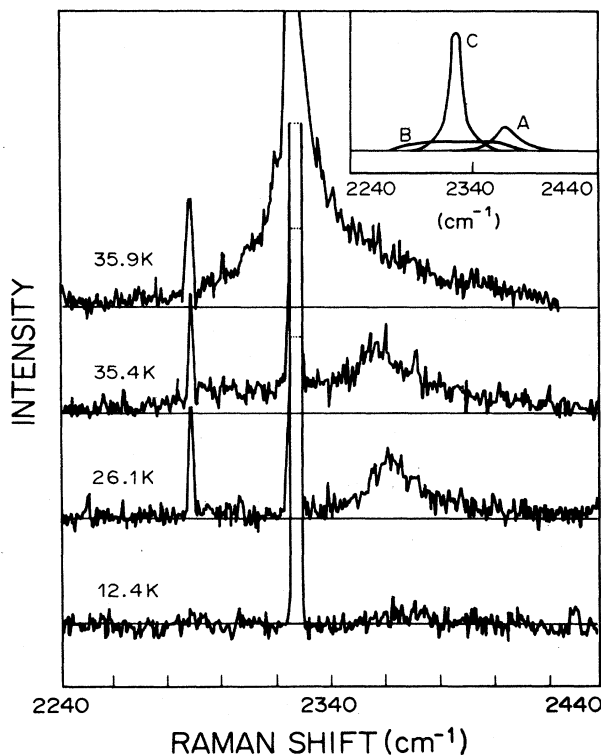


FIG. 3. The weak features of Fig. 2 for selected temperatures. Inset shows schematically the decomposition of *A*, *B*, and *C*.

clear from Fig. 4. The arrow points to the spectrum at  $T = T_c = 35.6 \text{ K}$ . A weak peak around  $60 \text{ cm}^{-1}$  (not evident on the intensity scale of Fig. 4) is the second  $T_g$  librational mode while the broad structures extending out to about  $100 \text{ cm}^{-1}$  are combination modes. As evident from Fig. 4(b), the librational modes merge as  $T_c$  is approached from below. We find that the librational  $E_g$  and  $T_g$  peaks, including the wings, display a behavior analogous to that of the  $A_g + T_g$  stretching mode. In particular, the maximum of the scattering cross section in the stretching and libration regions occurs in the temperature range  $26.1 < T < 34.6 \text{ K}$ .

In the  $\beta$  phase, the much broader modes near 25 and  $50 \text{ cm}^{-1}$  are the  $E_{2g}$  (phonon) and  $E_{1g}$  (librational) modes, respectively.<sup>1</sup> These observations are consistent with a precessing molecule model in the  $\beta$  phase.

#### IV. DISCUSSION AND CONCLUSIONS

As the phase boundary is crossed, there are changes in the Raman spectra that can be correlated and understood on the basis of the well-established structural transition  $\alpha \rightarrow \beta$ . For example the changes to the symmetry and frequency of the librational modes, that correlate with the translational order parameter, are consistent with the transition from cubic to hexagonal symmetry at  $T_c$  and have been reported earlier.

More specifically to the present work, we have found indirect evidence for the "plastic phase." Although predicted on the basis of molecular dynamics calculations,<sup>6</sup> this new phase that correlates with the orientational or-

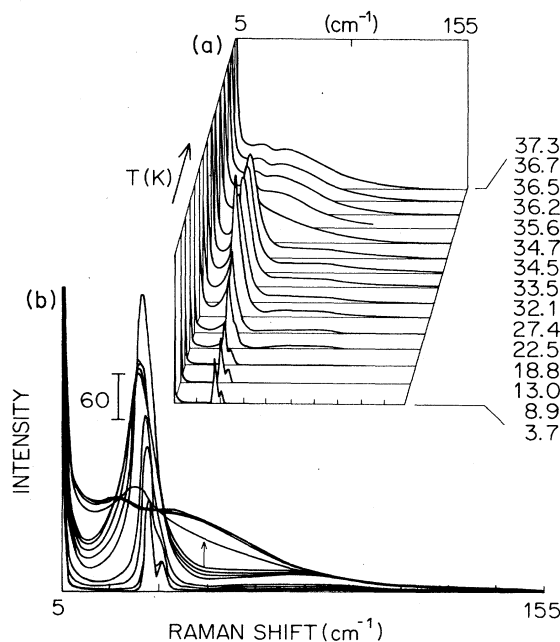


FIG. 4. (a) Evolution of the strongest low-frequency Raman modes as a function of temperature. (b) Superposed spectra illustrating the changes in position, shape and intensity. The maximum intensity is at 27.4 K. The number 60 on the vertical axis indicates the intensity relative to Figs. 2(a) and 2(b).

der parameter has not been experimentally identified. This parameter relates to the directional stability within the  $\alpha$  phase and is unity when the molecules in the primitive cell are perfectly oriented. Consistent with a partial relaxation of the molecular orientation is a broadening of the stretching and librational Raman modes. We identify this broadening with the gradual appearance of wings to the Raman line corresponding to the stretching mode in the  $\alpha$  phase several degrees below  $T_c$ —feature *B* of Fig. 2. The weakness of *B* and its increased intensity with temperature is in agreement with a partial orientational relaxation of the molecules. As the temperature is increased, one would expect the populations of the higher librational energy levels to increase. Moreover, because of anharmonicity their amplitudes should become large. In fact, the  $\alpha \rightarrow \beta$  transition may be viewed as a breakdown of the orientational order characterizing the  $\alpha$  phase due to the buildup of large amplitude librational motion of the molecules as a function of temperature. On crossing  $T_c$ , the stretching mode is further broadened as is evidenced in the feature *C*; this feature is consistent with the model of a transition from an orientationally ordered crystal to a fully disordered (precessional) phase.

In Fig. 4, depicting the lattice-mode energy region, wings to the librational modes are also evident, particularly on the low-frequency side. Again, consistent with a partial relaxation of the orientational order, is the appreciable increase in the intensity of the wings observed for temperatures 10 K below  $T_c$ . Significant changes in the ir spectra for temperatures a few degrees below  $T_c$  in the far-infrared region have also been reported.<sup>15</sup> To account for the linewidths of the  $E_g$  lattice mode at  $\sim 30 \text{ cm}^{-1}$ , we note however that it has been proposed that the libron could combine with another excitation to create a third mode, possibly an ir-active phonon.<sup>14</sup>

The second new result is the dramatic increase and

subsequent decrease in intensity with small temperature increases within the  $\alpha$  phase. At present, we have no satisfactory theoretical explanation for this behavior. These changes are very much larger than the ones expected due to variations in lattice constants or Boltzmann factors with temperature. In this respect, the spectra of solid  $\text{N}_2$  are very different from those of solid hydrogens<sup>16</sup> in which there are no unexplained changes in the intensities of the Raman lines with temperature. As is well known, solid hydrogens are quantum crystals in which the molecules rotate almost freely because of the relative weakness of anisotropic interactions. In contrast, in solid  $\text{N}_2$  the anisotropic interactions (most importantly the quadrupole-quadrupole interaction) are large in comparison to the rotational level spacings so that the molecules do not rotate freely; thus  $\text{N}_2$  can be considered to behave more like a classical solid. In fact, it is these interactions, which are so large at the lowest temperatures in the  $\alpha$  phase, that align the intermolecular axes leading to only a librational motion about the equilibrium sites.<sup>17</sup> We note that the dramatic changes in scattering intensity for small changes in temperatures are also greatest for temperatures approximately 10 K below  $T_c$ . It is at these temperatures when the wings in the Raman features appeared, signaling the orientational breakdown.

In summary, we have measured the Raman spectra of solid  $\text{N}_2$  crossing the  $\alpha$ - $\beta$  phase boundary at small temperature intervals. We find evidence for partial orientational relaxation in the  $\alpha$  phase about 10 K below  $T_c$ . This is consistent with the existence of a "plastic phase" that had been predicted over a decade ago with no experimental confirmation until now.<sup>6</sup> We also report a dramatic evolution of the Raman intensity with temperature within the  $\alpha$  phase. It will be interesting to investigate whether crystal dynamics<sup>18</sup> or molecular dynamics<sup>19</sup> calculations can account for this behavior.

\*Present address: Laboratoire d'Infrarouge, Associe au CNRS, Universite de Paris-Sud, Orsay CEDEX, France.

<sup>1</sup>T. A. Scott, *Phys. Rep.* **27**, 89 (1976).

<sup>2</sup>N. Jacobi and O. Schnepp, *J. Chem. Phys.* **57**, 2516 (1972).

<sup>3</sup>D. A. Goodings and M. Henkelman, *Can. J. Phys.* **49**, 2898 (1971).

<sup>4</sup>J. C. Raich, *J. Chem. Phys.* **56**, 2395 (1972).

<sup>5</sup>M. J. Mandell, *J. Chem. Phys.* **60**, 1432 (1974); **60**, 4880 (1974).

<sup>6</sup>B. Quentrec, *Phys. Rev. A* **12**, 282 (1975).

<sup>7</sup>A. B. Harris and C. F. Coll III, *Solid State Commun.* **10**, 1029 (1972).

<sup>8</sup>D. C. Wallace, *Thermodynamics of Crystals* (Wiley, New York, 1972).

<sup>9</sup>M. Brith, A. Ron, and O. Schnepp, *J. Chem. Phys.* **51**, 1318 (1969).

<sup>10</sup>J. E. Cahill and G. E. Leroi, *J. Chem. Phys.* **51**, 1324 (1969).

<sup>11</sup>A. Anderson, T. S. Sun, and M. C. A. Donkersloot, *Can. J.*

*Phys.* **48**, 2265 (1970).

<sup>12</sup>P. M. Mathai and E. J. Allin, *Can. J. Phys.* **49**, 1973 (1971).

<sup>13</sup>M. M. Thiery, D. Fabre, M. Jean-Louis, and H. Vu, *J. Chem. Phys.* **59**, 4559 (1973).

<sup>14</sup>F. D. Medina and W. B. Daniels, *J. Chem. Phys.* **64**, 150 (1976).

<sup>15</sup>G. Guelachvili, K. Narahari Rao, B. P. Winnewisser, M. Winnewisser, and R. H. Tipping, in *Recent Aspects of Fourier Transform Spectroscopy*, edited by G. Guelachvili, R. Kellner, and G. Zerbi (Springer-Verlag, Berlin, 1988).

<sup>16</sup>J. Van Kranendonk, *Solid Hydrogen* (Plenum, New York, 1983).

<sup>17</sup>J. C. Raich and R. D. Eters, *J. Low Temp. Phys.* **7**, 449 (1972).

<sup>18</sup>J. K. Kjems and G. Dolling, *Phys. Rev. B* **11**, 1639 (1975).

<sup>19</sup>D. Frenkel and J. P. McTague, *J. Chem. Phys.* **72**, 2801 (1980).